Spectral effects simulation with two-dimensional magnetohydrodynamic models of the solar photosphere

I. N. Atroshchenko and V. A. Sheminova

Main Astronomical Observatory, National Academy of Sciences of Ukraine
Zabolotnoho 27, 03689 Kyiv, Ukraine

Abstract

To study the structure of spatially unresolved features of the solar photosphere, we calculated the Stokes profiles of seven photospheric iron lines using two-dimensional nonstationary MHD models of solar granulation for various amounts of magnetic flux (0, 10, 20, 30 mT). We investigate variations in the absolute wavelength shifts and bisectors of the I profiles, as well as variations in the zero-crossing wavelength shifts, amplitude and area asymmetry of the V profiles as functions of magnetic field strength and time. The center-to-limb variations of the Stokes profiles are analyzed. The iron abundance is found to be 7.57, with the photosphere inhomogeneities taken into account. Although most of the spectral effects simulated within the scope of the two-dimensional MHD models are in satisfactory agreement with observational data, these models cannot always give a quantitative agreement. The absolute wavelength shifts of the Stokes profiles of Fe II lines calculated with the MHD models are substantially smaller than the observed ones.

1 Introduction

Our knowledge of the structure of small-scale magnetic features on the Sun is based mainly on spectroscopic observations in polarized light. To obtain the information from observations, we have to take recourse to laborious simulations of spectral effects. The simulation is made for such spectral line parameters which depend primarily on the properties of magnetic elements and can be easily interpreted. Nowadays we are able to study spatially unresolved magnetic elements with strong magnetic fields. A technique for the diagnostics of small-scale magnetic features has been elaborated quite well. Concurrent spectropolarimetric observations of several hundred lines are successfully carried out. Multidimensional MHD models of solar granulation are built. All these advances make it possible to calculate the Stokes profiles of spectral lines, compare them with observations, and gain information on the internal structure of magnetic flux tubes. The most interesting object of studies in the interpretation of the Stokes profiles is the V-profile asymmetry found in 1985 in observations of plages and the quiet Sun network [21, 24]. Up to now, no source has been found for the asymmetry of Stokes profiles (see overview [19]). While the mechanism of area asymmetry can be understood in general, the amplitude asymmetry may be caused by various factors (variations of velocity along and across the line of sight, time variations, etc.), and so we still do not understand what makes the V-profile amplitudes asymmetric even at the disk center. That is why any attempt to reproduce the observed asymmetry

using MHD models gives an additional valuable information on the structure of magnetic elements and their environment. A correct reproduction of the asymmetry is the most rigorous test for solar granulation models.

In this study we intended to calculate the Stokes profiles of photospheric lines using 2-D MHD models of the solar photosphere described in our paper [3], to study profile variations in time and in space depending on amount of magnetic flux and position on the solar disk, and thus to find whether such theoretical models can be used to interpret spectropolarimetric observations.

2 Model of the solar photosphere

Theoretical 2-D nonstationary MHD models of the solar photosphere [3] are characterized by a high spatial resolution (the horizontal calculation mesh width is 15 km), the existence of magnetic flux tubes in the region simulated, as well as the existence of nonmagnetic regions between the flux tubes – the granules. These models allow not only the simulation of spectral effects in the Stokes V profiles, but the analysis of I profiles as well, and this widens the scope of spectral analysis. Recall major features of these models.

We commonly assume in 2-D models that magnetic elements are either symmetric from the viewpoint of parallel transfer or axially symmetric. In the first case they are magnetic flux slabs, and in the second case they are magnetic flux tubes. Our models deal with flux slabs , but we call them flux tubes by convention. The simulated region comprises 256×128 calculation meshes with a horizontal and a vertical width of 15 km, it is rectangular in shape, 3840 km wide and 1920 km high, its upper boundary corresponds to the height $H = 600$ km above the level $\tau_R = 1$. The region may be considered as 256 vertical columns spaced at intervals of 15 km parallel to one another and to the line of sight. The location, thickness, and number of magnetic flux tubes in the simulated region depend on mean amount of magnetic flux and simulation time. The number of flux tubes and their width at the level $\tau_5 = 1$ increase with mean magnetic flux. The filling factor in the region grows with magnetic flux. The temperature in the flux tubes in the region of formation of spectral lines, i.e., above the level $\tau_5 = 1$, increases as compared to the surrounding nonmagnetic medium. The intensity of the continuous radiation emerging from flux tubes also increases. The maximum magnetic field strength in flux tubes is approximately the same in all models ($B = 200$ mT at $\tau_5 = 1$). The Wilson depression is 150–200 km.

Comparing the temperature $<T>$ averaged over space and time for our MHD models and the temperature T for the quiet photosphere (the empirical homogeneous HOLMU model), we found that $<T>$ for a theoretical nonstationary nonmagnetic model was higher than T, the excess being as large as 400 K in the region where weak lines are formed ($\log \tau_5 = -0.5$) and several tens of degrees in the region where moderate-strong lines are formed. The space-average temperature for MHD models slightly diminishes with growing simulation time at a particular mean field strength. The temperature $<T>$ diminishes as well with increasing mean field strength in the simulated region.

We used four model sequences in the Stokes profile calculations, the mean magnetic field strengths in them were 0, 10, 20, and 30 mT, each sequence had five models calculated for points of 21, 22, 23, 24, and 25 min in time. In all, we had twenty 2-D models. The model for a specific mean strength (for instance, 10 mT) and a specific point in time (for instance, 25 min) is designated as MHD-10-25.

3 Calculating the Stokes profiles

The transfer equations for a radiation polarized in a magnetic field were solved separately for every model column. First the optical depth τ_5 in the continuum along the line of sight was determined, and then the Stokes profiles were calculated in the LTE approximation by the procedure described by Beckers [4] and Landi Degl'Innocenti [12]. The algorithm and program for the Stokes profile calculations are described in detail by Sheminova [14, 15]. The mesh for solving the equations of transfer along the line of sight was built in the following manner. The initial mesh point (the point on the upper boundary of simulated region where the radiation emerges on the solar surface) was found from the model values of the geometric height H, continuous absorption coefficient κ_5, and matter density p which correspond to two points in the model beginning from the upper boundary of the region: $\tau_5 = 1/2(H_2 - H_1)[(\kappa_5\rho)_1 + (\kappa_5\rho)_2]$ according to the trapezoidal formula. Then all subsequent points $\tau_n = \tau_{n-1} + 1/2(H_n - H_{n-1})[(\kappa_5\rho)_n + (\kappa_5\rho)_{n-1}]$. Thus the model values of H were scaled to the τ_5 scale and then to the $\log\tau_5$ scale. After that, we specified a standard mesh nonuniform in $\log\tau_5$: $\log\tau_5$ was 0.2, 0.15, 0.1, 0.05, and 0.1 in the intervals between $\log\tau_5$ values of -6.4, -5.2, -4.0, -3.0, -0.5, and 1.0. All model parameters were calculated according to the standard mesh, and our experience suggests that the mesh gives stable results. The number of mesh points did not exceed 95. The models were calculated for various distances from the disk center with $\cos\theta$ taken into account. The models were thus made ready for exact calculations of the transfer equations of Unno-Beckers-Landi Degl'Innocenti.

The Stokes profiles were calculated for each column, then they were averaged over the simulated region, and we got a profile for a particular magnetic flux and a particular point in time. As we had five models for points in time 21, 22, 23, 24, and 25 min, we had five corresponding profiles. We averaged them over time and found a resulting profile for a specific magnetic flux, and this profile could be compared with observations which have a low spatial and temporal resolution. To study the center-to-limb variations in the Stokes profiles, the calculations were made for five values of $\cos\theta = 0.3$, 0.45, 0.67, 0.83, 1.0. We picked the optimum horizontal mesh width which would provide the necessary accuracy with shortest computing time. Calculations of a profile averaged over time and over columns with mesh widths of 15, 30, 45, 60, and 90 km suggested that the optimum mesh width was 60 km, and thus we worked with 64 columns rather than with 256.

3.1 Selected spectral lines

We selected seven lines which are often used in observations of magnetic features. Table 1 gives their atomic parameters: the low excitation potential χ_e, effective Landé factor $g_{\rm eff}$, oscillator strength $\log gf$ from [5] (and from [23] for the line Fe I λ 526.06 nm and for Fe II lines), effective optical depths of formation of the profile center and the whole profile – $\log\tau_d$ and $\log\tau_W$. The damping constant was calculated with Unsold's formula. The lines were selected so that the photospheric region where they are formed might be as extended as possible. As is evident from the effective line formation depths calculated with the depression contribution functions for the quiet Sun [9], the lines selected by us refer to that region in the photosphere which extends from $\log\tau_5 = -1$ to $\log\tau_5 = -3$, and therefore all results of our spectral analyses refer to just this part of the photosphere. The number of lines was limited mainly by great time expenditure in the Stokes profile calculations for the MHD models.

The observational data we used in this study were taken from various investigations

Table 1: Lines used in the analysis

Ion	λ, nm	χ_e, eV	$g_{\rm eff}$	$\log gf$	$\log \tau_d$	$\log \tau_W$
Fe I	524.70585	0.09	2.00	-4.946	-2.65	-2.05
Fe I	525.02171	0.12	3.00	-4.938	-2.60	-2.02
Fe I	525.06527	2.20	1.50	-2.120	-3.15	-2.09
Fe II	614.92490	3.89	1.33	-2.850	-1.05	-0.88
Fe I	615.16220	2.18	1.83	-3.299	-1.78	-1.50
Fe I	617.33410	2.22	2.50	-2.880	-2.26	-1.75
Fe II	643.26830	2.89	1.83	-3.760	-1.22	-1.00

published already. The observed Stokes profiles for three lines obtained with a high spatial and temporal resolution in plages near the solar disk center were taken from paper [1]. The entrance slit was 0.5″ and the exposure time 0.2–0.5 s in those observations. The center-to-limb variations in the amplitude, asymmetry, and profile parameters were observed with a 5″ slit and an exposure time of 43–72 min [22]. These two observation series differ basically by their spatial and temporal resolution. We used observations of other authors as well.

3.2 Calculation scheme

All parameters in our self-consistent MHD models are interdependent. Chemical abundance and damping constant are the only free parameters in the profile calculations. Therefore, the first stage in the calculations was to determine these parameters for every spectral line by fitting the equivalent widths and/or central depths of the I profiles calculated with the MHD models with a zero magnetic flux to those observed for the quiet Sun as given in atlas [7]. The second stage was to calculate the Stokes profiles for every line with the abundance and damping constant found for that specific line and with the MHD models with a magnetic field. Then the profile parameters were calculated – bisectors, absolute wavelength shifts, amplitude and area asymmetry, zero-crossing wavelength shifts, peak separation, amplitude ratios for pairs of lines, etc. The third stage was to compare the calculation results with observations.

4 Analysis of the calculated Stokes I profiles for the quiet Sun

4.1 Iron abundance

The iron abundance determined by us is given in Table 2, where d and W are the central depth and the equivalent width of I profiles measured in atlas [7], H_d and H_W are the effective geometric height of line core formation and the weighted average effective height over the whole profile calculated in [9] for the HOLMU model, A_d, A_W are the iron abundances obtained by fitting central depths and equivalent widths; ΔA_{W-d} is the difference between the abundances A_W and A_d. The differences ΔA calculated with the MHD-0 models are in good agreement with those found in [9] with the HOLMU model, except for strong lines, for which the difference becomes greater.

Several factors are responsible for the discrepancy between A_W and A_d. The damping constant may be one of them. To verify this assumption, we introduced a correction factor E in the calculations ($\gamma = E\gamma_{\rm VdW}$). We calculated the profiles with various correction values ($E = 1,\ 2,\ 3$) and found that the abundance errors caused by uncertainty in

Table 2: Iron abundance

λ, nm	d	W, pm	H_W, km	H_d, km	A_W	A_d	ΔA_{W-d}	ΔA_{W-d} [9]
524.70585	0.716	6.036	328	415	7.48	7.65	-0.17	-0.11
525.02171	0.710	6.490	324	409	7.58	7.65	-0.07	-0.03
525.06527	0.793	10.400	330	493	7.52	7.39	-0.13	-0.08
614.92490	0.347	4.030	132	164	7.63	7.52	0.11	0.10
615.16220	0.507	4.858	235	283	7.62	7.68	-0.06	-0.06
617.33410	0.622	6.930	279	361	7.55	7.58	-0.03	-0.02
643.26830	0.364	4.190	159	194	7.64	7.56	0.08	0.06
Average					7.57	7.57		

the damping constant were 0.02 dex for our lines, and their effect on A_W and A_d was unimportant. We believe that temperature is the most probable factor for the differences between A_W and A_d. Gurtovenko and Sheminova [10] demonstrated that these differences could be successfully used for improving solar model photospheres. Now we try to test the MHD-0 model using the abundances A_W and A_d obtained. If the model temperature is lower than the actual temperature in the region of line formation, W and d for moderate Fe I lines in this model are greater than the observed W and d and, therefore, we get A_W and A_d smaller than the actual iron abundance, and vice versa, i.e., the following relationships hold true: if $T_{\rm mod} < T$, $A_d < A$ and $A_W < A$; if $T_{\rm mod} > T$, $A_d > A$ and $A_W > A$. As the spectral lines have different atomic parameters, they react in different ways on temperature changes, and so we divided the lines into three groups: moderate-weak wide lines Fe II 614.92, 643.26 nm; moderate narrow lines Fe I 525.02, 524.70, 615.16, 617.33 nm; moderate-strong wide line Fe I 525.06 nm. According to quantitative estimates by Sheminova [17], the same temperature fluctuations ΔT produce a weak response in the lines in the first group and a strong response in the second group, while the lines in the third group demonstrate an intermediate response. The central depths are more responsive in narrow lines, and equivalent widths in broad lines. We derived the average iron abundances $A_d = 7.55$, $A_W = 7.64$ from Fe II lines (the first group), $A_d = 7.64$, $A_W = 7.54$ from Fe I lines in the second group, and $A_d = 7.39$, $A_W = 7.52$ in the third group. The results for the first two groups are explicable if we assume that the average temperature in the simulated region is higher than the actual temperature and the difference ΔT need be only 20–50 K in the region of formation of moderate Fe I lines and 200–400 K in the region of formation of Fe II lines. The strong photospheric line in the third group is formed in the most extended region, which embraces virtually all photospheric layers. As a result the effective layers of formation of the line core may lie very close to the upper boundary of MHD models in those model regions where the absorption increases, and then the abundance A_d is more distorted than A_W or than A_d from moderate lines. Since the MHD models are truncated and temperature fluctuations can be quite appreciable in the upper layers, this seems to be the reason why the abundances A_d were found smaller than A_W.

Exact determination of iron abundance is still an open problem (see review [11]). Analysis of the A_W and A_d obtained by us indicates that the average temperature is likely to be slightly overestimated in the MHD models in the region where moderate Fe I lines are formed and is too high in the region where Fe II lines are formed. Calculations and analyses of strong photospheric Fe I lines with our MHD models cannot give reliable results because the models are truncated in the upper photosphere. Nonetheless the average iron abundances A_W and A_d derived from all lines by fitting the calculated central depths and equivalent widths to observed ones coincide and are 7.57 with rms errors of ± 0.06 for A_W and 0.12 for A_d. This iron abundance is close to that in meteorites (7.55).

Table 3: Doppler shift (in units of m/s)

Quiet Sun				Magnetic regions						
$\Delta\lambda_I$				$\Delta\lambda_I$			$\Delta\lambda_V$			
λ, nm	0.4, pm	0.1, pm	[8]	10	20	30, mT	10	20	30, mT	[1]
524.70	-143	57	-81	76	145	180	560	280	116	–
525.02	-137	63	-133	59	131	171	548	319	162	–
525.06	-120	91	-179	131	221	245	471	365	211	–
614.92	-195	5	-1108	-88	84	134	1400	496	302	495
615.16	-146	19	-387	15	95	138	860	371	171	530
617.33	-146	-9	-203	38	129	163	703	414	231	420
643.26	-140	19	-491	-57	103	143	1225	575	282	–
Average	-146	35	–	25	129	147	824	482	218	–

4.2 Absolute wavelength shifts of I profiles

Absolute Doppler shifts $\Delta\lambda = c(\lambda_c - \lambda)/\lambda$ calculated for I profiles are given in Table 3. We found the central wavelength λ_c for a displaced profile as the center of gravity of the area of I-profile core, for the profile section cut off by a line at half-maximum intensity. The wavelength λ_c was found to be very sensitive to the method of its determination and to the wavelength step $\Delta\lambda$ within the profile. Table 3 gives the shifts $\Delta\lambda$ calculated from profiles with the steps $\Delta\lambda = 0.4$ pm and $\Delta\lambda = 0.1$ pm. We found that the Doppler shift could not be determined more accurate than to 0.1 pm, and this results in an error of 50 m/s. The observed absolute shifts $\Delta\lambda$ are taken from study [8]. It is well known that line shifts are caused by convective motions of matter. Negative shifts point to upward motions toward the observer (blue shifts), positive shifts suggest that the matter moves downward from the observer (red shifts). The absolute line shifts calculated with our MHD models are too small as compared to observations and are almost the same.

4.3 Bisectors of I profiles

Bisectors are usually used to indicate the asymmetry of I profiles. The absolute shift of bisectors characterizes the velocity amplitude, and their bend characterizes the velocity gradient. We have to keep in mind, however, that the bisector shape is affected by temperature structure changes to a greater extent than by velocity (see review [2]). The results obtained in our study are illustrated by bisectors for three lines in Fig. 1. All the bisectors are C-shaped. The greatest blue bend in the bisectors of stronger lines is smaller than the observed bend. The calculated bisectors are shifted only slightly with respect to the observed ones.

So, the calculations of I profiles and their parameters reveal that MHD models for the quiet Sun describe adequately the observed spectral effects and reproduce the well-known relationships, but a quantitative checking suggests that the model is slightly "overheated", and this is likely to be the cause of small absolute shifts derived by us. To test this assumption, we studied the variations of the calculated central depths $d_c = 1 - I/I_c$, equivalent widths W, and absolute shifts $\Delta\lambda_I$ along the region simulated with a zero field strength for points in time 21–25 min. We selected two lines, λ 614.9 nm ($H_d \approx$ 150 km) and λ 525.02 nm ($H_d \approx 400$ km), in order to follow the parameter variations at different photospheric levels. The line λ 525.02 nm being highly sensitive to temperature, the dependence of its central depth on distance x along the region has sharp dips at the boundaries of granules and intergranular lanes, where the temperature rises. The

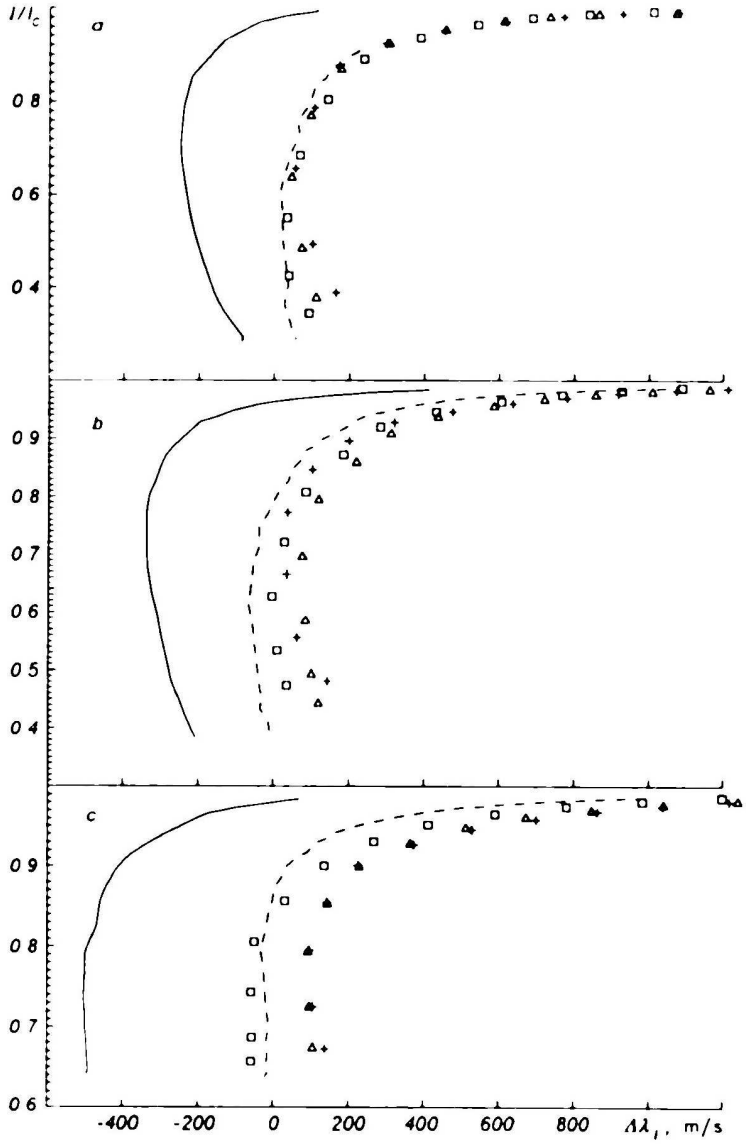

Fig 1. I-profile bisectors on the absolute-shift scale; a) Fe I λ 524.7 nm, b) Fe I λ 617.3 nm, c) Fe II λ 643.2 nm. Solid line) observations, dashed line) MHD-0, squares) MHD-10, triangles) MHD-20, plusses) MHD-30.

equivalent widths follow in general the run of $d_c(x)$, but there are some peculiarities. The relations $d_c(x)$ and $W(x)$ account for temperature variations in the region, and $\Delta\lambda_1(x)$ accounts in full measure for variations in vertical velocity. Figure 2 displays the absolute shifts along the length of the region simulated by MHD-0. The shift $\Delta\lambda_1$ is predominantly positive in intergranular lanes and negative in granules, thus allowing a clear delineation between granules and integranular lanes. We observed no significant difference in the changes of $\Delta\lambda_1(x)$ for both lines at different photospheric levels. Oscillations of vertical velocities in time can be seen in granules, but we could not detect 5-min oscillations, probably because of a long temporal step (1 min). The absolute shifts calculated for the profiles averaged over the region at the moments 21, 22, 23, 24, 25 min are 517, 5, -51, -127, -316 m/s (λ 614.9 nm) and 794, -167, 55, -161, -347 m/s (λ 525.02 nm), and for the profiles averaged also in time they were 4 m/s (λ 614.9 nm) and 60 m/s (λ 525.02 nm). These shifts are substantially smaller than the observed shifts, especially for the line Fe II λ 614.9 nm. A shift of -133 m/s observed in λ 525.02 nm is attained in the calculations at some moments, but a shift of -1108 m/s observed in the λ 614.9 nm line has not been reached at all. We may infer that the time averaging is a very delicate element in simulating absolute shifts. It has to be done either over a long time interval or with

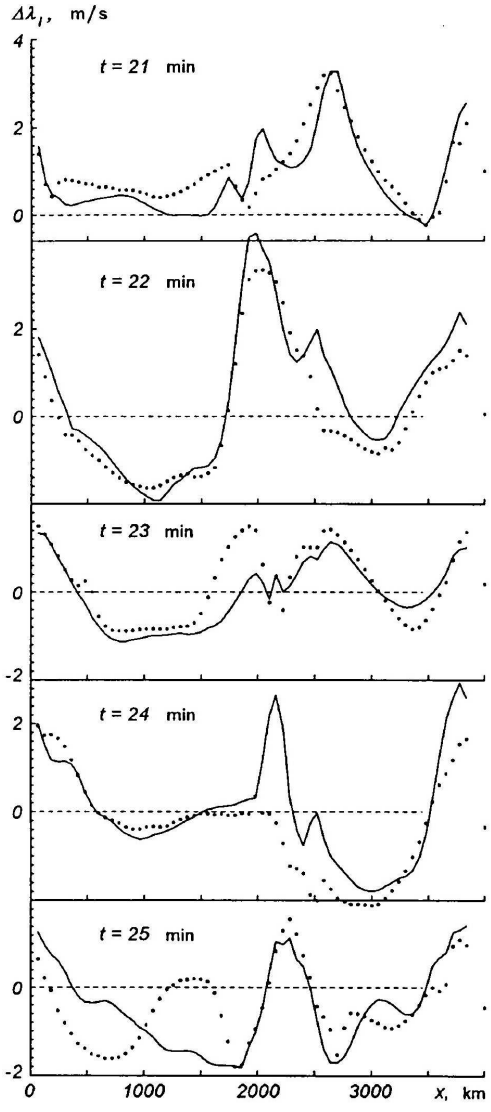

Fig.2. Variations in the absolute shifts along the length of the region simulated with a zero field strength (model MHD-0). Solid line) λ 614.9 nm, dots) λ 525.02 nm.

a small time step. There may exist another cause of small shifts in the region of Fe II line formation. Observations indicate that the pattern of convective motions changes in the middle photosphere, the correlation between brightness and velocity is violated. Blue absolute shifts become very small at a height of about 300 km and become even red above this level. Below, at a height of 100 km, blue shifts increase up to 1.5–2 km/s. It is likely that our models simulate inadequately the violation of the brightness–velocity relationship, and so the gradient of vertical velocities in the models is too low. The cause appears to be a too large line opacity coefficient, which results in a slower cooling of the matter than in the actual solar photosphere.

5 Analysis of the Stokes profiles calculated for active features

Profiles of the Stokes parameters I, Q, U, and V offer considerable scope for studying physical conditions in small-scale magnetic features. The diagnostics of magnetic fields is made primarily with the Q, U, and V profiles of some infrared lines [13] and V profiles of lines in the visible region, and with the use of the method of V-profile amplitude ratios

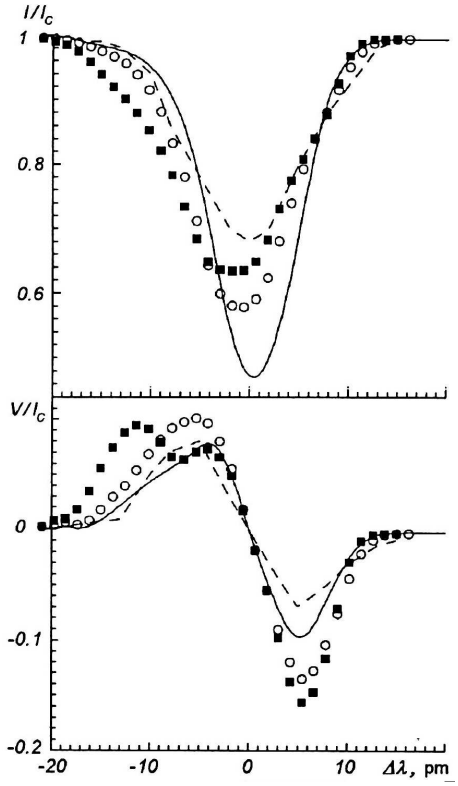

Fig. 3. The Stokes I and V profiles of the line Fe I λ 617.33 nm calculated for the MHD-30 model. Solid line) entire region simulated, circles) magnetic flux tube region 1800–2800 km, dark squares) magnetic flux tube region 2200–2600 km, dashed line) observations with high spatial resolution [1].

for pairs of lines [20] or center-to-limb variations in the V-profile parameters [22]. The diagnostics of velocities in magnetic elements is made by measuring zero-crossing shifts, broadening and asymmetry of V profiles. The zero-crossing shift $\Delta\lambda_V$ is measured with respect to the wavelength of the core center of I profile (λ_c), i.e., $\Delta\lambda_V = \lambda_V - \lambda_c$, λ_V being the wavelength of the V-profile center. The V-profile center is a point in the profile where it crosses the λ-axis, passing from its blue wing to the red wing. The wavelength of the I-profile center λ_c is defined as a point where $d(I/I_c)/d\lambda = 0$ rather than the center of gravity of the profile core. The V-profile broadening is defined by the full width at half-maximum (FWHM) of the blue and red wings and by the difference $\Delta\lambda_a$ between the blue and red wing maxima. The V-profile asymmetry is measured by the parameters $\delta a_V = (a_b - a_r)/(a_b + a_r)$ and $\delta A_V = (A_b - A_r)/(A_b + A_r)$, a and A being the amplitude and area of the blue (b) and red (r) wings (they are usually taken without sign). The temperature diagnostics in spatially unresolved magnetic elements is done from the Q, U, and V profiles of strong lines and also with the use of the V-profile amplitude ratio between two lines with different temperature response.

5.1 The Stokes I and V profiles

Observed I and V profiles (with large $a_b,\ a_r$) can be found in paper [1], they were obtained for three lines (Fe I 615.1 nm, 617.3 nm, Fe II 614.9 nm) in the plage regions $0.63''$ in size, the observation time was 0.5 s. The lines Fe II 614.9 nm and Fe I 615.1 nm were observed simultaneously in an active plage near a spot at $\cos\theta = 0.953$, and the line Fe I 617.3 nm was observed in another intense plage near a spot at $\cos\theta = 0.866$. We compared these profiles with calculated profiles averaged over the entire simulated region (about $7''$) and over time (5 min). The mean field strength in this region was 30 mT. No Stokes profiles calculated with our models could fit the observed profiles. Then we calculated anew the profiles for the Fe I λ 617.3 nm line, having changed the spatial averaging. We selected two

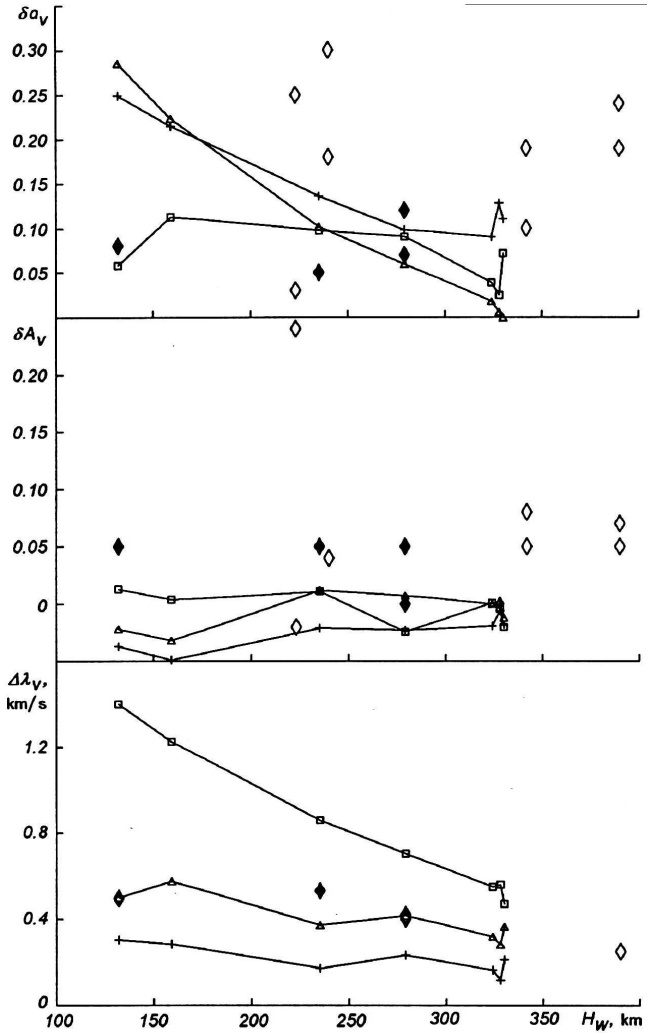

Fig. 4. Amplitude asymmetry δa_V and area asymmetry δA_V, and zero-crossing wavelength shift $\Delta\lambda_V$ as functions of formation height for seven iron lines with the models MHD-10 (plusses), MHD-20 (triangles), and MHD-30 (squares). Dark diamonds) high-resolution observations [1], light diamonds) low-resolution observations [18].

areas 1.5″ and 0.6″ in size from the simulated region with a stronger magnetic flux tube located at the center of these areas (region 2 in Fig. 3 [3]). Thus we increased substantially the filling factor. Figure 3 displays the I and V profiles averaged over time for the entire region (0–3840 km), for the entire region 2 (1800–2800 km), and for the central part of region 2 (2200–2600 km). The results of our calculations confirmed the assumption of Amer and Kneer [1] that the filling factor is of great importance for the cases considered. Time variations in the profile do not reproduce the observed weakening of I profiles, while spatial changes of the region seem to account for the observed effect. Notice that the $\Delta\lambda$ zero-point in Fig. 3 coincides with the zero-crossing wavelength λ_V for the V profiles, just as this was done in [1].

5.2 Amplitude and area asymmetry and zero-crossing wavelength shifts of the V profiles

Figure 4 shows the asymmetry of amplitudes (δa_V) and areas (δA_V) as well as zero-crossing wavelength shifts ($\Delta\lambda_V$) derived for V profile calculated with MHD models and observed taken from the literature. The calculated profiles were obtained for three regions at the disk center with mean field strengths of 10, 20, and 30 mT, the time interval was 21–25 min. The effective heights H_W of formation of each V profile were taken from Table 2. Our calculations [16] indicate that the heights H_W calculated with a magnetic field and

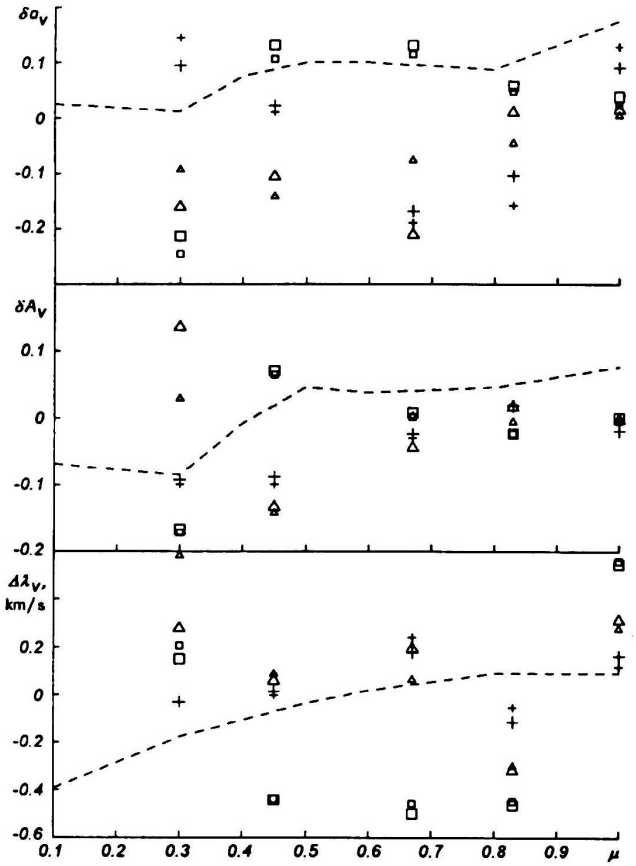

Fig. 5. Center-to-limb variations in the amplitude asymmetry δa_V, area asymmetry δA_V, and zero-crossing shift $\Delta\lambda_V$ for MHD-10 (squares), MHD-20 (triangles), MHD-30 (plusses). Larger marks) line λ 525.02 nm, smaller marks) λ 524.7 nm.

without it are practically the same. Besides, the effective heights for I and V profiles differ insignificantly. As can seen from Fig. 4, the calculated amplitude asymmetry fits quite well the measurements in plages with high spatial resolution [1], while the calculated area asymmetry is systematically smaller than the observed one. The area asymmetry varies from 0 to 0.08 as measured by various observers and from -0.05 to 0.02 in our calculations, i.e., our models do not reproduce the observed area asymmetry δA_V. The zero-crossing shifts $\Delta\lambda_V$ derived for simulated regions with a mean field strength of 20 mT are in accord with observations made with a high spatial resolution [1]. As regards the absolute shifts of I profiles (see Table 2), our calculations do not reveal any blue shift as we have already noted for the region with a zero magnetic flux. The absolute shifts $\Delta\lambda_I$, averaged over all lines were found to be 35, 25, 129, 147 m/s for mean magnetic fluxes of 0, 10, 20, 30 mT, respectively. One can see that the effect of shift "reddening" with growing filling factor does really exist. Brandt and Solanki [6] measured $\Delta\lambda_I$ = -223, -125, -104, -164 m/s for different filling factors – $\alpha < 1\%$, $1\% \leq \alpha < 4\%$, $4\% \leq \alpha < 8\%$, or $\alpha \geq 8\%$ respectively. Thus, we may infer that the simulated asymmetry and shift parameters follow the general trends observed in the behavior of these parameters. The calculated V-profile amplitude asymmetry and zero-crossing shift fit observations. The fact that we derived underestimated parameters for the V-profile area asymmetry and absolute shifts of I profiles suggests that the velocity field structure in the MHD models [3] is inadequate.

Figure 5 illustrates the behavior of the calculated amplitude asymmetry δa_V, area asymmetry δA_V, and zero-crossing shift $\Delta\lambda_V$ as functions of μ, the position of the simulated region on the disk. Low-resolution observations of V profiles of the lines Fe I 524.7, 525.02 nm [22] are shown by dashed lines, the data were averaged over many plages which differed by their filling factors. Our calculations were made for three regions with 10,

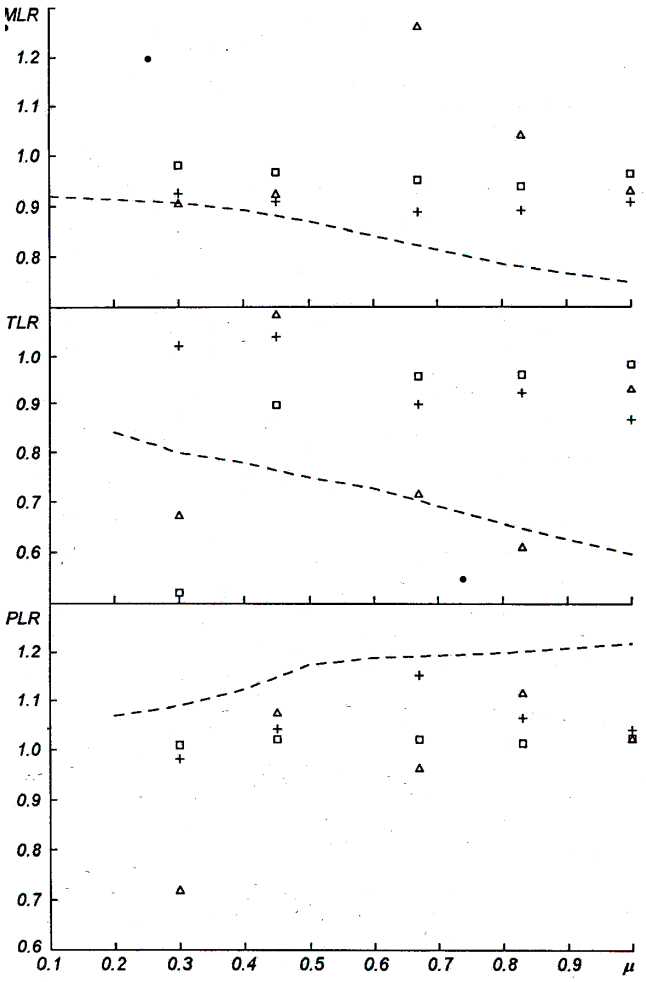

Fig. 6. The Stokes V-amplitude magnetic (MLR), temperature (TLR) line ratios, and the Stokes V peak separation line ratio (PLR) as functions of position on the solar disk (μ) for MHD-10 (squares), MHD-20 (triangles), MHD-30 (plusses). Dashed line represents observations [22].

20, and 30 mT in the time interval 21–25 min, for different values of μ. The calculated dependence of δa_V, δA_V, $\Delta\lambda_V$, agrees satisfactorily with the observed one. For $\mu = 1$ the asymmetry parameters of both lines Fe I 524.7, 525.02 nm are smaller than the observed asymmetry parameters.

5.3 Line ratios

Figure 6 shows the magnetic line ratios MLR = $a_{V,\,525.02}/1.5a_{V,\,524.70}$, the Stokes V peak separation line ratios PLR = $\Delta\lambda_{a,\,525.02}/\Delta\lambda_{a,\,524.72}$, and the temperature line ratios TLR = $a_{V,\,524.70}/0.75a_{V,\,525.06}$ calculated by us for different values of μ, the observed ratios [22] are also given. The relations MLR(μ) and PLR(μ), which provide information on the magnetic field gradient, indicate that the calculated ratios MLR are higher than the observed ones, especially at the center of the disk. The ratios must grow toward the limb if B decreases with height, but our data suggest that this effect is weak. It is likely that the field gradient in the flux tubes simulated is lower than in actual flux tubes in the region of formation of these lines. The calculated PLR values are smaller than the observed ones: the effect is the same as for the V-profile amplitude ratios discussed above.

To study the temperature stratification in small-scale magnetic elements, we selected the lines Fe I 525.06, 524.7 nm. The first line being stronger than the second one, $a_{V\,525.06}$ for it is smaller by 13% as compared to $a_{V,\,524.70}$, and therefore TLR ≈ 1.15 at the center of the disk and TLR ≈ 1 at the limb. Deviations from these values specify the temperature variation in flux tubes. Observations [22] give the value TLR < 1.15. This means that

the line becomes weaker in a flux tube owing to a temperature increase with respect to a nonmagnetic environment. The deviation from unity diminishes toward the limb – the temperature difference ΔT between the flux tube and the medium decreases. As can be seen in Fig. 6, the calculated values of TLR are higher than the observed ones. This suggests that ΔT in the simulated areas are smaller as compared to actual temperature conditions observed in plages.

The results obtained with the line-ratio method indicate that the magnetic field strength gradients and the temperature distribution in flux tubes are not reproduced adequately by our MHD models. Observations require larger gradients and higher temperatures.

6 Conclusion

Simulation of spectral effects in the Stokes profiles with the use of multidimensional MHD models demonstrates once again that construction of such models is of prime importance for the interpretation of spectra with the aim to study the structure of the atmospheres of the Sun and stars. The simulation of spectral effects in V profiles carried out earlier with 1-D models of magnetic flux tubes proved to be incapable of adequate representation of observations. Asymmetry is not reproduced in the one-dimensional approximation (e.g., see [18]). The two-dimensional simulation employed in this study improved considerably the qualitative results, though it is still far from the desired performance. The principal results of this study are as follows.

1. The iron abundance derived from the equivalent widths and central depths of selected spectral lines is 7.57 ± 0.10.

2. The bisectors of I profiles are C-shaped. The blue bend of bisectors in moderate-strong lines is smaller than the observed one.

3. We obtained smaller absolute wavelength shifts, especially for Fe II lines. For instance, the observed shifts $\Delta\lambda_I$ for the lines Fe I λ 525.02 nm, Fe II λ 614.9 nm are -133 and -1108 m/s, while the calculated shifts are 63 and 5 m/s. The calculated absolute shifts "redden" with growing mean field strength in the region simulated, just as the observed shifts do.

4. The amplitude asymmetries calculated for the V profiles of the lines studied, δa_V, fit satisfactorily the observations made with high temporal and spatial resolution, they range from 0 to 0.3. The deeper the line is formed, the greater is the asymmetry δa_V, while no direct dependence on magnetic field strength is found.

5. The asymmetry of V-profile areas was found to be smaller than the observed one – our calculations give δA_V from -0.05 to 0.02, while the observed values range from 0 to 0.08. The asymmetry δA_V grows with field strength and is virtually independent of the line formation height.

6. The zero-crossing shifts in V profiles relative to I profile are larger for the lines which form deeper in the photosphere, they also increase with magnetic flux. For regions simulated with mean field strengths of 10, 20, 30 mT we derived shifts (averaged over all lines) of 824, 482, 218 m/s, respectively, while low-resolution observations in the plages usually produce shifts of about 200 m/s and high-resolution observations in the plages give about 400 m/s. The agreement may be considered as quite satisfactory.

7. The Stokes profiles as well as their temperature and magnetic ratios calculated as function of height in the photosphere and position on the solar disk reproduce qualitatively the tendencies observed in the behavior of these parameters, but the quantitative estimates are not consistently in agreement.

Our final inference is that our models are "overheated" in the upper photosphere and as a consequence the gradients of velocities and magnetic field are underestimated. We believe that the overheating is caused by a too high opacity coefficient in lines, and in addition, the simulation results for the upper layers are strongly affected by boundary conditions. Thus, the synthesis of spectral effects is a rather rigorous test for MHD models. On the other hand, further improvement of numerical simulation methods advances our understanding of the physical processes responsible for the formation of small-scale magnetic elements and the observational spectral effects related to them.

Acknowledgements. We thank A. S. Gadun for useful comments and advice. The study was partially financed by the Joint Foundation of the Government of Ukraine and the International Science Foundation (Grant No. K111100) and by the European Southern Observatory (Grant No. A-01-009).

References

[1] M. A. Amer and F. Kneer, "High spatial resolution spectro-polarimetry of small-scale magnetic elements on the Sun," Astron. and Astrophys., vol. 273, no. 1, pp. 304–312, 1993.

[2] I. N. Atroshchenko, A. S. Gadun, S. I. Gopasyuk, et al., Variations in the Global Characteristics of the Sun [in Russian], pp. 182–231, Naukova Dumka, Kyiv, 1991.

[3] I. N. Atroshchenko and V. A. Sheminova, "Numerical simulation of the interaction between solar granulation and small-scale magnetic fields," Kinematika i Fizika Nebes. Tel [Kinematics and Physics of Celestial Bodies], vol. 12, no. 4, pp. 32–45, 1996.

[4] J. M. Beckers, "The profiles of Fraunhofer lines in the presence of Zeeman splitting. I. The Zeeman triplet," Solar Phys., vol. 9, no. 2, pp. 372–386, 1969.

[5] D. E. Blackwell, M. J. Shallis, and G. I. Simmons, "Note on the interpretation of Fe I lines (2.18-2.49 eV) in the solar spectrum," Mon. Notic. Roy. Astron. Soc., vol. 199, no. 1, pp. 33–36, 1982.

[6] P. N. Brandt and S. K. Solanki, "Solar line asymmetries and the magnetic filling factor," Astron. and Astrophys., vol. 231, no. 1, pp. 221–234, 1990.

[7] L. Delbouille, L. Neven, and G. Roland, Photometric Atlas of the Solar Spectrum from 3000 to 10000 A, Lie'ge, 1973.

[8] D. Dravins, L. Lindegren, and A. Nordlund, "Solar granulation: Influence of convection on spec tral line asymmetries and wavelength shift," Astron. and Astrophys., vol. 96, no. 1/2, pp. 345–364, 1981.

[9] E. A. Gurtovenko and R. I. Kostyk, The Fraunhofer Spectrum and the System of Solar Oscillator Strength [in Russian], Naukova Dumka, 1989.

[10] E. A. Gurtovenko and V. A. Sheminova, "On a possibility of improving the homogeneous model of the solar photosphere," Kinematika i Fizika Nebes. Tel [Kinematics and Physics of Celestial Bodies], vol. 4, no. 3, pp. 18–23, 1988.

[11] R. I. Kostik, N. G. Shchukina, and R. J. Rutten, "The solar iron abundance: not the last word," ibid., vol. 305, no. 1, pp. 325–342, 1995.

[12] E. Landi Degl'Innocenti, "MALIP – a programme to calculate the Stokes parameter profiles of magnetoactive Fraunhofer lines," Astron. and Astrophys. Suppl. Sen, vol. 25, pp. 379–390, 1976.

[13] K. Mudlach and S. K. Solanki, "Infrared lines as probes of solar magnetic features. I. A many-line analysis of a network region," Astron. and Astrophys., vol. 263, no. 1/2, pp. 301–311, 1992.

[14] V. A. Sheminova, Calculating the Profiles of the Stokes Parameters of Magnetoactive Absorption Lines in Stellar Atmospheres [in Russian], Kyiv, 1990 (VINITI File No. 2940-V90, 30 May 1990).

[15] V. A. Sheminova, Effect of Physical Conditions in the Medium and of Atomic Constants on the Stokes Profiles of Absorption Lines in the Solar Spectrum [in Russian], Kyiv, 1991 (Institute of Theoretical Physics AS Ukr SSR Preprint ITF-90-87P).

[16] V. A. Sheminova, "Depths of formation of magnetically sensitive absorption lines in the solar atmosphere," Kinematika i Fizika Nebes. Tel [Kinematics and Physics of Celestial Bodies], vol. 8, no. 3, pp. 44–62, 1992.

[17] V. A. Sheminova, "Parameters of sensitivity of Fraunhofer lines to changes in the temperature, gas pressure, and microturbulent velocity in the solar photosphere," ibid., vol. 9, no.5, pp. 27–43, 1993.

[18] S. K. Solanki, "The origin and the diagnostic capabilities of the Stokes V asymmetry observed in solar faculae and the network," ibid., vol. 224, no. 1/2, pp. 225–241, 1989.

[19] S. K. Solanki, "Small-scale solar magnetic fields: an overview," Space Sci. Revs., vol. 63, pp. 1–188, 1993.

[20] J. 0. Stenflo and J. W. Harvey, "Dependence of the properties of magnetic fluxtubes on area factor or amount of flux," Solar Phys., vol. 95, no. 1, pp. 99–118, 1985.

[21] J. 0. Stenflo, J. W. Harvey, J. W. Brault, and S. K. Solanki, "Diagnostics of solar magnetic fluxtubes using a Fourier transform spectrometer," Astron. and Astrophys., vol. 131, no, 2, pp. 333–346, 1984.

[22] J. O. Stenflo, S. K. Solanki, and J. W. Harvey, "Center-to-limb variation of Stokes profiles and the diagnostics of solar magnetic fluxtubes," ibid. vol. 171, no. 1/2, pp. 305–316, 1987.

[23] F. Thevenin, "Oscillator strengths from the solar spectrum," Astron. and Astrophys. Suppl. Sen, vol. 77, pp. 137–154, 1989.

[24] E. Wiehr, "Spatial and temporal variation of circular Zeeman profiles in isolated solar Ca K structures," Astron. and Astrophys., vol. 149, no. 1, pp. 217–220, 1985.